Strongly Interacting Photons in 2D Waveguide QED

Matija Tečer,[1] Marco Di Liberto,[1,2,3] Pietro Silvi,[1,2,3] Simone Montangero,[1,2,3] Filippo Romanato,[1,2,4] and Giuseppe Calajó[3]

[1]*Dipartimento di Fisica e Astronomia "G. Galilei", via Marzolo 8, I-35131 Padova, Italy*
[2]*Padua Quantum Technologies Research Center, Universitá degli Studi di Padova*
[3]*Istituto Nazionale di Fisica Nucleare (INFN), Sezione di Padova, I-35131 Padova, Italy*
[4]*CNR-IOM Istituto Officina dei Materiali, Trieste, Italy*

(Received 13 December 2023; revised 28 February 2024; accepted 11 March 2024; published 15 April 2024)

One-dimensional confinement in waveguide quantum electrodynamics (QED) plays a crucial role to enhance light-matter interactions and to induce a strong quantum nonlinear optical response. In two or higher-dimensional settings, this response is reduced since photons can be emitted within a larger phase space, opening the question whether strong photon-photon interaction can be still achieved. In this study, we positively answer this question for the case of a 2D square array of atoms coupled to the light confined into a two-dimensional waveguide. More specifically, we demonstrate the occurrence of long-lived two-photon repulsive and bound states with genuine 2D features. Furthermore, we observe signatures of these effects also in free-space atomic arrays in the form of weakly subradiant in-band scattering resonances. Our findings provide a paradigmatic signature of the presence of strong photon-photon interactions in 2D waveguide QED.

DOI: 10.1103/PhysRevLett.132.163602

The capability of engineering effective photon-photon interactions is a compelling requirement in many quantum technology applications for the generation and manipulation of complex states of light [1]. This task has been successfully achieved in light-matter interfaces, such as cavity QED [2], Rydberg atomic ensembles [3–5] and waveguide QED [6,7], where nonlinear quantum optical effects are strongly enhanced. In particular, waveguide QED has recently emerged as a versatile and experimentally implementable platform where the light confined in a 1D channel, either at optical [8–11] or microwave frequencies [12–16], couples to one or multiple quantum emitters. In this scenario, light confinement leads to strong photon correlations, resulting in antibunched [17,18] or bunched output photons [17,19–24]. Among the causes of the bunching phenomena is the emergence of multiphoton bound states [17,20,23,25] where two or more photonic excitations propagate jointly in the system with spatially correlated positions. Remarkably, the lifetime and the dispersion properties of these states can be enhanced when ordered atomic arrays are coupled to the waveguide [26–30] or to waveguide networks [31,32]. In this setting, the realized bound state can be interpreted as a propagating excitation, which acts as a moving defect in the otherwise periodic medium, dragging other photons with it. The recent progress in building scalable microwave resonator arrays coupled to superconducting qubits [33–35], in interfacing 2D photonic crystals with cold [36] or artificial atoms [8,37,38] and quantum emitters interacting with atomic matter waves [39–41] have created new experimentally viable opportunities for studying QED in 2D confined geometries. This scenario is particularly fascinating when combined with the possibility to induce photon-photon interactions and to build strongly correlated many-body quantum phases of light [42,43].

In this Letter, we show that photonic states exhibiting both spatial repulsion and binding can occur by coupling a 2D atomic array to light confined into a 2D photonic structure (see Fig. 1). The emergence of such strong interactions in this 2D environment represents a nontrivial outcome. Indeed, unlike the 1D scenario, where photon-mediated interactions among emitters are infinite-range, in two dimensions, they decay as the square root of the

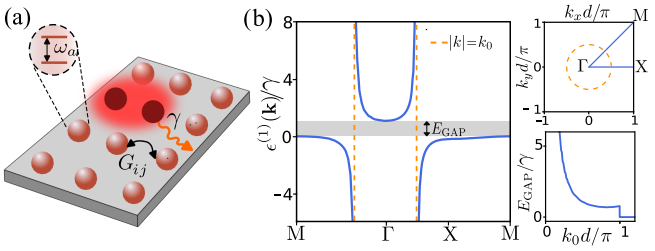

FIG. 1. (a) A square array of two level atoms is coupled to the light confined into a 2D photonic waveguide. (b) Single photon dispersion relation for $k_0 d = (\pi/2)$. Upper right panel: first Brillouin zone and Γ, X, M symmetry points. Lower right panel: Band gap energy as a function of the interatomic distance $k_0 d$. The gap closes at $k_0 d > \pi$. The dashed orange lines indicate the dispersion's divergences at $|\mathbf{k}| = k_0$.

emitters separation. We show that the interacting photonic states occurring in the system possess a distinct 2D structure, exhibiting binding and repulsion along different directions. Their existence is made possible by an interference process originating from the 2D collective interaction of the emitters and does not rely on the engineering of the photonic bath [44–47]. Furthermore, we identify metastable in-band localized scattering resonances. Notably, these states also manifest in free-space atomic arrays, expanding the range of platforms where our findings can be explored [48–50]. Finally, we demonstrate how to excite the photon bound states via a dynamical relaxation process. Our results provide a realistic pathway for realizing strongly correlated states of light in 2D confined geometries in the subwavelength regime.

Model.—We consider a two-dimensional square array of N two-level atoms with ground and excited states $|g\rangle$, $|e\rangle$ and lattice constant d perfectly coupled [51] to the light confined into a 2D waveguide, as shown in Fig. 1. To simplify the description of this complex light-matter interacting system we integrate out the photonic degrees of freedom employing a Born-Markov approximation. This procedure is valid as long as the atom-photon dynamics, which is set by the atomic decay rate γ, occurs on a timescale slower than a photon freely propagating through the whole array. We obtain an effective spin model for the atoms described by the non-Hermitian Hamiltonian ($\hbar = 1$) [6,52–54]

$$\hat{H}_{\text{eff}} = \sum_{ij} G(k_0|\mathbf{x}_i - \mathbf{x}_j|)\hat{\sigma}_+^i \hat{\sigma}_-^j, \tag{1}$$

where $k_0 = 2\pi/\lambda$ is the photon wave vector whose corresponding frequency is resonant with the atomic transition frequency ω_a and $\hat{\sigma}_+^i = |e\rangle\langle g|$ and $\hat{\sigma}_-^i = (\hat{\sigma}_+^i)^\dagger$ are the pseudospin operators for the ith atom located at the position $\mathbf{x}_i$. The dissipative and coherent long-range photon-mediated interactions among the atoms are encoded in the function $G(k_0|\mathbf{x}_i - \mathbf{x}_j|)$, related to 2D electromagnetic Green's function of the nanophotonic structure [54]. For confined photons with a quadratic isotropic dispersion relation, it reads $G(z) = (\gamma/2)[\mathcal{Y}_0(z) - i\mathcal{J}_0(z)]$ [51,55–58]. Here $\mathcal{J}_0(z)$ and $\mathcal{Y}_0(z)$ are, respectively, the zeroth order Bessel functions of the first and second kind, which decay as $z^{-1/2}$. The Hamiltonian in Eq. (1) provides a complete description of the system within a fixed excitation sector in the absence of an external pumping field. For a single excitation, the Hamiltonian is diagonalized by Bloch waves, labeled by the wave vector $\mathbf{k}$, having eigenvalues $E^{(1)}(\mathbf{k}) = \epsilon^{(1)}(\mathbf{k}) - i\gamma^{(1)}(\mathbf{k})/2$, where $\epsilon^{(1)}(\mathbf{k})$ and $\gamma^{(1)}(\mathbf{k})$ provide the single-excitation dispersion relation and collective decay rates, respectively [51]. The dispersion relation (Fig. 1) exhibits two distinct polaritonic branches, along with a band gap near the atomic resonance frequency, where propagation of excitations is forbidden. Differently from 1D wQED [6,29], the band gap closes for interatomic distances above the subwavelength regime (see Fig. 1), $k_0 d > \pi$, namely, for $d > \lambda/2$, due to the occurrence of higher diffraction orders. Note that, similar to 1D wQED [29,59], the divergences in the dispersion relation at the resonant wave vector, $|\mathbf{k}| = k_0$, are associated with superradiant modes [59–61].

Interacting photons.—To demonstrate that strong photon-photon interactions occur in this 2D setting, we consider the two-body problem described by Eq. (1) restricted to the two excitations subspace. We focus on the thermodynamic limit of an infinite array, where there are no channels of dissipation and the spectra is real and determined by the coherent part of Hamiltonian (1). By reparametrizing the arrangement of the atoms in terms of center-of-mass ($\mathbf{R}$) and relative ($\mathbf{r}$) coordinates, we reduce the two-body problem to a single-particle one for the relative coordinate space and described by the basis set $|\mathbf{K}, \mathbf{r}\rangle$, where the parametric dependence on the center-of-mass momentum $\mathbf{K}$ is explicitly indicated [51]. The corresponding Hamiltonian matrix elements read

$$(\hat{H}_{\text{eff}})^{\mathbf{K}}_{\mathbf{r},\mathbf{r}'} = \sum_{\epsilon=\pm} \cos\big(\mathbf{K}/2 \cdot (\mathbf{r} + \epsilon\mathbf{r}')\big)\mathcal{R}\{G(k_0|\mathbf{r} + \epsilon\mathbf{r}'|)\}, \tag{2}$$

where $\mathcal{R}$ denotes the real part. Numerical diagonalization returns the two-body spectrum, $\epsilon^{(2)}(\mathbf{K})$, plotted in Fig. 2(a). We observe a continuum of unbound two-particle states, whose energies correspond to the sum of two single-particle excitations, separated by a band gap hosting a dispersive state. Most of the continuum states away from the high-symmetry points of the Brillouin zone (BZ) are scattering states made of a pair of particles with relatively high group velocity (see Fig. 1), thus experiencing a weak mutual interaction [6]. Instead, close to those high-symmetry points, the relatively flat single-particle dispersion can provide an enhancement of interactions. It is convenient to map the matrix elements in Eq. (2) onto a single-particle model for the relative coordinate $\mathbf{r}$ in the presence of an impurity potential, described by the Hamiltonian:

$$\hat{H}^{(\text{imp})}_{\mathbf{K}} = \sum_{\mathbf{r}\mathbf{r}'} J^{\mathbf{K}}_{\mathbf{r}\mathbf{r}'} |\mathbf{K}, \mathbf{r}\rangle\langle \mathbf{K}, \mathbf{r}'| + U|\mathbf{K}, 0\rangle\langle \mathbf{K}, 0|, \tag{3}$$

where the first term describes free particle propagation, while the second term implements the short-range impurity potential with infinite strength, $U \to \infty$, located at $\mathbf{r} = 0$. Here the hopping coefficient is $J^{\mathbf{K}}_{\mathbf{r}\mathbf{r}'} = (1/N)\sum_{\mathbf{q}} \epsilon^{(2)}_{\text{scat}} \times (\mathbf{K}, \mathbf{q}) e^{i(\mathbf{r}-\mathbf{r}')\mathbf{q}}$, where $\mathbf{q}$ is the relative momentum and the dispersion is given by the sum of individual photon energies, $\epsilon^{(2)}_{\text{scat}}(\mathbf{K}, \mathbf{q}) = \epsilon^{(1)}(\mathbf{q}) + \epsilon^{(1)}(\mathbf{K} - \mathbf{q})$. The effective model of Eq. (3) is obtained by reformulating the Hamiltonian (1) in terms of hardcore bosons and then solving again the two-body problem in the relative coordinate frame [51]. In this way, the hardcore photon-photon interactions are mapped to

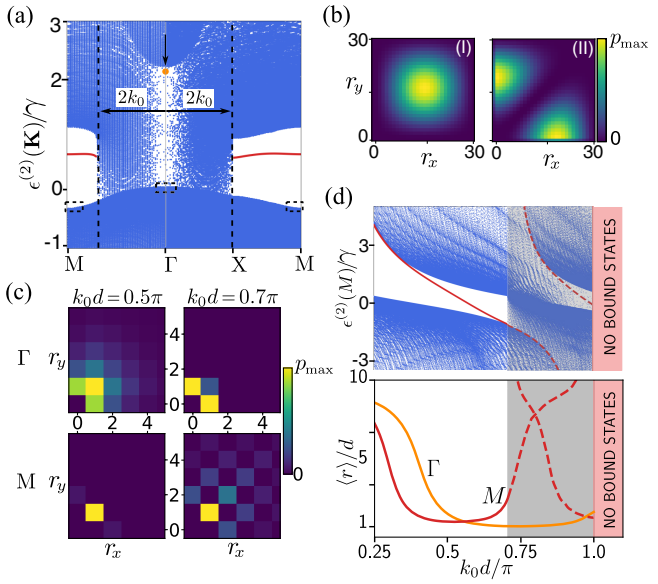

FIG. 2. (a) Two-excitation spectrum as a function of the center-of-mass momentum for $k_0d = (\pi/2)$. Blue dots represent unbound states while the red lines and the orange dot represent the bound states. The dashed black boxes indicate the regions where the repulsive states lie. (b) Relative coordinate population distribution, $p(r_x, r_y)$, of two kinds of repulsive states at the Γ point for $k_0d = 0.5$. Similar distributions up to a phase modulation are observed at the M point. (c) Zoom of the bound states distribution at Γ and M point for $k_0d = 0.5\pi, 0.7\pi$. (d) Two-excitation spectrum at the M point (upper panel) and average relative distance between two excitations, $\langle r \rangle$, (lower panel) as a function of k_0d. The continuous lines indicate the BSs while the dashed ones in the gray area indicate the scattering resonances branches.

the impurity term of Eq. (3), which reflects the saturation of an atom after the absorption of one excitation.

The first consequence of strong photon interactions originating from the hard-wall condition induced by the impurity potential is the presence of two kinds of *repulsive* scattering states indicated by the black dashed squares in Fig. 2(a). Their population distribution in the relative coordinate shows a smooth repulsion of the two excitations either with respect to the $r_x = 0$ and $r_y = 0$ axis (type I) or with respect to the $r_x = r_y$ diagonal (type II), as shown in Fig. 2(b). The 1D analog of these states have been recently discussed both in free space [54] and wQED atomic arrays [59,60,62–66] and are commonly referred to as "fermionic" states.

Besides repulsive states we also identify the presence of photon-photon bound states (BSs) [17,20,23,25–29]. Here the two excitations are spatially correlated and their occurrence can be understood, within the impurity model (3), in terms of a defect bound state localized around $\mathbf{r} = \mathbf{0}$. The BSs energy, $E_{\mathrm{BS}}(\mathbf{K})$, indicated by the red lines of Fig. 2(a), can be computed by using Green's function methods [51,67] and it is given by the numerical solution of $\mathcal{G}_0[0, E_{\mathrm{BS}}(\mathbf{K})] = 1/U$ for $U \to \infty$, with

$$\mathcal{G}_0(\mathbf{r}, E) = \frac{1}{(2\pi)^2} \int_{\mathrm{BZ}} d^2\mathbf{q} \frac{e^{i\mathbf{q}\cdot\mathbf{r}}}{E - \epsilon^{(2)}_{\mathrm{scat}}(\mathbf{K}, \mathbf{q})}, \tag{4}$$

being the free particle Green's function. The BSs solutions need to respect the constraint $E_{\mathrm{BS}}(\mathbf{K}) \neq \epsilon^{(2)}_{\mathrm{scat}}(\mathbf{K}, \mathbf{q})$, meaning that their occurrence is conditioned to the existence of a band gap in the relative coordinate space. This requirement is not matched for $k_0d > \pi$ due to the closing of the single-excitation gap in two dimensions discussed before (see Fig. 1), which prevents the gap formation also for the two-particle spectrum. For $k_0d < \pi$, a gap in $\epsilon^{(2)}_{\mathrm{scat}}(\mathbf{K})$ exists for values of the center-of-mass momentum in the range $|\mathbf{K}| > 2k_0$ within the BZ. This condition cannot be satisfied within the BZ when $2k_0$ becomes equal to the M point momentum, $|\mathbf{K}_M| = \sqrt{2}\pi/d$, and the gap therefore closes [51]. An additional gap occurs exactly at the Γ point due to a perfect vanishing of the density of states [28,29] and persists for all interatomic distances $k_0d < \pi$.

Once we established the conditions of existence of the BSs, we can use the impurity model to compute the bound states population distribution, $p(\mathbf{r}) = |\mathcal{G}_0[\mathbf{r}, E_{\mathrm{BS}}(\mathbf{K})]|^2$, in the relative coordinate space. An example is shown in Fig. 2(c) for the Γ and M points at two different interatomic distances. These plots clearly show a pronounced localization in the vicinity of $\mathbf{r} = 0$, meaning that the two excitations are bound and spatially correlated. We quantify this binding by the average distance between two excitations, $\langle r \rangle = \sum_{\mathbf{r}} p(\mathbf{r})|\mathbf{r}|$, which strongly depends on the inter-atomic distance, k_0d, as shown in Fig. 2(d). The plot shows how the bound states at Γ and M points are largely extended at short interatomic distances and progressively become more localized. The Γ point BS experiences minimal extension at the interatomic distance of $k_0d \sim 0.74\pi$, where a destructive interference process induced by the effective impurity is enhanced along the nearest neighbor direction [26]. When such an interference process is tailored along the next-nearest neighbor direction, the BS changes its relative coordinate distribution accordingly [see the first row of Fig. 2(c)]. This occurs at $k_0d \approx 0.74/\sqrt{2}\pi \approx 0.52\pi$. The behavior of the M point BS can be inferred from the center-of-mass momentum induced cosine modulation in Eq. (2). Such modulation effectively creates a sublattice with spacing $\sqrt{2}d$. The minima of the two curves in the lower panel of Fig. 2(d) are indeed displaced by such a factor, and the underlying modulation is visible in the bound state wave function shown in Fig. 2(c). At $k_0d = \pi/\sqrt{2}$ the M point gap closes and the BS ceases to exist. Nevertheless, we can still identify the presence of two localized states in the band, which can be interpreted as scattering resonances, states that contain both unbound and bound-state

contributions [28,51,68,69], whose energies and localization are shown in Fig. 2(d). Interestingly, close to $k_0 d = \pi$, we observe the formation of a region with low density of states [see Fig. 2(d)]. This mechanism depends on the shape of the dispersion relation and plays the role of an effective gap, for a finite size system, thus stabilizing them into quasibound states.

Interacting states lifetime.—The states described so far, being derived in the thermodynamic limit, have vanishing decay rates. In realistic settings, where the atomic lattice has a finite size, these states acquire a finite lifetime due to leakage of the excitations at the array's edges. The decay rate of these states is provided by the imaginary part of the two-excitation sector eigenvalues, $\gamma_s^{(2)}$, obtained via exact diagonalization of Eq. (1) [36,59], where s labels the different states. For both repulsive and bound states, the decay rates are much smaller than the single atom emission rate, γ, indicating a subradiant behavior. We find that, while the Γ point BSs have a weak dependence with the interatomic distance, the M point BSs, the associated scattering resonance and the repulsive states strongly depend on that. For both Γ and M point bound states the largest lifetime is achieved around $k_0 d \approx 0.52\pi$, resembling the localization plot shown in Fig. 2(d). At this atomic distance, the decay rates of the Γ and M point BSs scale approximately as $\sim N^{-1.5}$, as shown in Fig. 3. The different amplitude of the two BSs decay rates depends from a larger localization of the M photon bound state in the center-of-mass coordinate induced by a quasi-flat dispersion [27,51]. The repulsive states exhibit an even stronger subradiant behavior with a scaling of $\sim N^{-3}$, which reflects the one of two independent single-excitation states [51,54]. These findings demonstrate that long-lived photon interacting states can occur even for finite size arrays.

Free space array.—Some of the discussed interacting states can be probed also in the absence of a photonic structure by considering a 2D free space subwavelength atomic array. [70–75]. By fixing for simplicity the atomic polarization to be orthogonal to the array's plane, the projected dyadic Green's function ruling the atomic interactions in Eq. (1) reads [51,54,76–78]: $G(x) = (3\gamma_0)/[4(k_0 x)^3] e^{ik_0 x}(1 - ik_0 x - (k_0 x)^2)$, where $\gamma_0 = d_{eg}^2 k_0^3/(3\pi\hbar\epsilon_0)$ is the free space spontaneous emission decay rate with d_{eg} being the dipole moment strength. In this scenario there is no band gap in the single-excitation subspace and therefore neither in the two-excitations subspace. Thus, no BSs can form in this setting. However, it is still possible to identify two-excitation scattering resonances exhibiting a localized wave function in their relative coordinate. For these states, we pinpoint regions characterized by a low density of states, where they become metastable within the subradiant region $k_0 d < \sqrt{2}\pi$ [51]. This is illustrated in Fig. 3 by the scaling of subradiant decay rates at the Γ and M points, exhibiting dependencies of $N^{-1.2}$ and $N^{-0.7}$, respectively. It

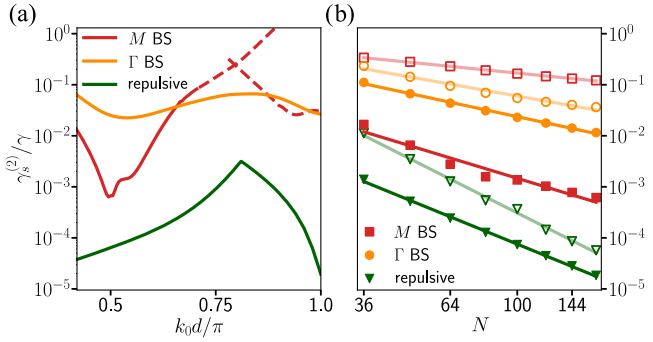

FIG. 3. (a) Decay rates $\gamma_s^{(2)}$ of the interacting states as a function of $k_0 d$ for an array of $N = 10 \times 10$ atoms. (b) Finite size scaling of the decay rates γ_s with the system size N in the 2D waveguide case (filled symbols) compared to the free space scenario (empty symbols). Here we fixed $k_0 d = 0.52\pi$ for the 2D waveguide while $k_0 d = 1.09\pi$ and $k_0 d = 0.73\pi$ for the Γ and M point in the free space case. In both plots, we considered as repulsive state the type II one.

is noteworthy that these states can endure in the system for a timescale more than 10 times greater than that associated with the decay of a single atom. In addition to these localized states, we also identify the presence of repulsive states presenting a similar decay rate scaling as the ones for a 2D waveguide. Note that, without the challenges related to the interfacing of the atoms to a photonic structure (see Ref. [51]), these interacting excitations could potentially already be observed in current experimental implementations of subwavelength-ordered atomic arrays [48–50].

Dynamical excitation.—To observe the manifestation of BSs in the system dynamics, we consider a relaxation scenario where two atoms are initially excited in a configuration that has a large overlap with the target state. Specifically, we consider the dynamical excitation of the M point BS by exciting two atoms in the bulk of the system separated by a distance $\mathbf{x}_i - \mathbf{x}_j = \boldsymbol{\ell} = (\ell, \ell)$, $|\psi(t=0)\rangle = \hat{\sigma}_+^{\mathbf{i}} \hat{\sigma}_+^{\mathbf{i}+\boldsymbol{\ell}} |0\rangle$. For an interatomic distance of $k_0 d \approx 0.52\pi$ and an excitation separation of $\ell = 1$, this configuration has indeed a large initial overlap with the population distribution of the M point BS [51]. In Fig. 4 we plot the two excitation probability distribution in the relative and lab space coordinates at different times for this initial configuration. Since the dominant contribution comes from the M point BSs, the two excitations remain localized in their relative position during the evolution, while the BSs center of mass can diffuse across the lattice. As a measurable observable to detect the dynamical excitation of the BS we define the two particle equal time correlator $C_{\boldsymbol{\ell}}(t) = \sum_{\mathbf{i}} \langle \psi(t) | \hat{n}_{\mathbf{i}} \hat{n}_{\mathbf{i}+\boldsymbol{\ell}} | \psi(t) \rangle / |\langle \psi(t) | \psi(t) \rangle|^2$, where the vector index $\mathbf{i} = (i_x, i_y)$ spans the whole array, $\hat{n}_{\mathbf{i}} = \hat{\sigma}_+^{\mathbf{i}} \hat{\sigma}_-^{\mathbf{i}}$ and the denominator normalizes this quantity with respect to the probability of having two excitations in the system. This correlator indicates how likely is to find two excitations at a relative distance $\boldsymbol{\ell} = (\ell, \ell)$ in the entire array. Its

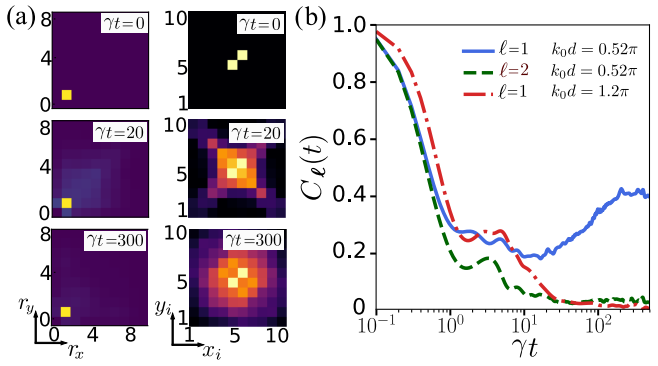

FIG. 4. (a) Two-excitation probability distribution in the relative (left panel) and lab coordinate (right panel) space at times $\gamma t = 0$, 20, 300 for $\ell = 1$ and $k_0 d = 0.52\pi$. (b) Time evolution of the two-particle correlator, $C_\ell(t)$, for different interatomic distances $k_0 d$ and different initial populations ($\ell = 1$, 2). For all figures we fixed $N = 10 \times 10$.

time evolution is plotted in Fig. 4 for different initial conditions. In particular, we consider the case $\ell = 1$, the one having a large overlap with the BS, and $\ell = 2$. In the first case, the two excitations stay bound together, as signaled by a persistent correlation at long times, whereas in the second case, the correlator quickly drops to zero. A large dropping is also observed, for an interatomic distance of $k_0 d \approx 1.2\pi$, where BSs do not exist. Note that a dynamical procedure similar to the one presented for the BSs could be employed to excite scattering resonances either in a 2D waveguide or in free space.

Conclusions and outlook.—We have discussed the emergence of two-photon strongly correlated and long-lived states in a 2D array of atoms coupled to a two-dimensional waveguide. Using a spin model formulation, we have characterized these states discussing their dispersion, binding and decay properties and we have demonstrated their manifestation in the system dynamics. The occurrence of these states crucially relies on interfacing an array of two-level atoms with the light confined into a two-dimensional photonic structure, but some of the discussed features could persist also in free space atomic arrays. This work opens interesting possibilities to study many-body physics with photons in this open and dissipative system. In particular, similarly as studied in 1D waveguide QED [23,29], we could expect the existence of multiphoton bound states and a "quantum to classical" transition toward the formation of 2D solitons [79,80]. Targets of ongoing investigation include exploring few-body interacting topological states [81–89] in atomic arrays [90–92] and emergent many-body phases in frustrated lattices [93,94]. Another interesting perspective is to investigate the occurrence of high-dimensional bound states in 3D atomic arrays [95,96] where the atomic lattice completely fills the electromagnetic environment.

This work was supported by the EU QuantERA2017 project QuantHEP, the EU QuantERA2021 project T-NiSQ, the Quantum Technology Flagship project PASQuanS2, the NextGenerationEU project CN00000013, the Italian Research Center on HPC, Big Data and Quantum Computing, the Quantum Computing and Simulation Center of Padova University, the INFN project QUANTUM, the Italian Ministry of University and Research (MUR) via PRIN2022-PNRR project TANQU, the Rita Levi-Montalcini program and via the Departments of Excellence grant 2023-2027 "Quantum Frontiers" (FQ) and by the project STRADA (Italian Presidency of the Council of Ministers).

[1] D. E. Chang, V. Vuletić, and M. D. Lukin, Nat. Photonics **8**, 685 (2014).
[2] A. Reiserer and G. Rempe, Rev. Mod. Phys. **87**, 1379 (2015).
[3] O. Firstenberg, C. S. Adams, and S. Hofferberth, J. Phys. B **49**, 152003 (2016).
[4] O. Firstenberg, T. Peyronel, Q.-Y. Liang, A. V. Gorshkov, M. D. Lukin, and V. Vuletić, Nature (London) **502**, 71 (2013).
[5] Q.-Y. Liang, A. V. Venkatramani, S. H. Cantu, T. L. Nicholson, M. J. Gullans, A. V. Gorshkov, J. D. Thompson, C. Chin, M. D. Lukin, and V. Vuletić, Science **359**, 783 (2018).
[6] A. S. Sheremet, M. I. Petrov, I. V. Iorsh, A. V. Poshakinskiy, and A. N. Poddubny, Rev. Mod. Phys. **95**, 015002 (2023).
[7] D. Roy, C. M. Wilson, and O. Firstenberg, Rev. Mod. Phys. **89**, 021001 (2017).
[8] P. Lodahl, S. Mahmoodian, and S. Stobbe, Rev. Mod. Phys. **87**, 347 (2015).
[9] J. D. Hood, A. Goban, A. Asenjo-Garcia, M. Lu, S.-P. Yu, D. E. Chang, and H. J. Kimble, Proc. Natl. Acad. Sci. U.S.A. **113**, 10507 (2016).
[10] N. V. Corzo, J. Raskop, A. Chandra, A. S. Sheremet, B. Gouraud, and J. Laurat, Nature (London) **566**, 359 (2019).
[11] A. Tiranov, V. Angelopoulou, C. J. van Diepen, B. Schrinski, O. A. D. Sandberg, Y. Wang, L. Midolo, S. Scholz, A. D. Wieck, A. Ludwig, A. S. Sørensen, and P. Lodahl, Science **379**, 389 (2023).
[12] O. Astafiev, A. M. Zagoskin, A. A. Abdumalikov, Y. A. Pashkin, T. Yamamoto, K. Inomata, Y. Nakamura, and J. S. Tsai, Science **327**, 840 (2010).
[13] J. D. Brehm, A. N. Poddubny, A. Stehli, T. Wolz, H. Rotzinger, and A. V. Ustinov, npj Quantum Mater. **6**, 10 (2021).
[14] M. Mirhosseini, E. Kim, X. Zhang, A. Sipahigil, P. B. Dieterle, A. J. Keller, A. Asenjo-Garcia, D. E. Chang, and O. Painter, Nature (London) **569**, 692 (2019).
[15] B. Kannan, A. Almanakly, Y. Sung, A. Di Paolo, D. A. Rower, J. Braumüller, A. Melville, B. M. Niedzielski, A. Karamlou, K. Serniak, A. Vepsäläinen, M. E. Schwartz, J. L. Yoder, R. Winik, J. I.-J. Wang, T. P. Orlando, S. Gustavsson, J. A. Grover, and W. D. Oliver, Nat. Phys. **19**, 394 (2023).
[16] P. S. Shah, F. Yang, C. Joshi, and M. Mirhosseini, arXiv:2402.15701.

[17] J.-T. Shen and S. Fan, Phys. Rev. A **76**, 062709 (2007).
[18] B. Schrinski and A. S. Sørensen, New J. Phys. **24**, 123023 (2022).
[19] J.-T. Shen and S. Fan, Phys. Rev. Lett. **98**, 153003 (2007).
[20] H. Zheng, D. J. Gauthier, and H. U. Baranger, Phys. Rev. Lett. **107**, 223601 (2011).
[21] S. Mahmoodian, M. Čepulkovskis, S. Das, P. Lodahl, K. Hammerer, and A. S. Sørensen, Phys. Rev. Lett. **121**, 143601 (2018).
[22] A. S. Prasad, J. Hinney, S. Mahmoodian, K. Hammerer, S. Rind, P. Schneeweiss, A. S. Sørensen, J. Volz, and A. Rauschenbeutel, Nat. Photonics **14**, 719 (2020).
[23] S. Mahmoodian, G. Calajó, D. E. Chang, K. Hammerer, and A. S. Sørensen, Phys. Rev. X **10**, 031011 (2020).
[24] H. Le Jeannic, A. Tiranov, J. Carolan, T. Ramos, Y. Wang, M. H. Appel, S. Scholz, A. D. Wieck, A. Ludwig, N. Rotenberg, L. Midolo, J. J. García-Ripoll, A. S. Sørensen, and P. Lodahl, Nat. Phys. **18**, 1191 (2022).
[25] N. Tomm, S. Mahmoodian, N. O. Antoniadis, R. Schott, S. R. Valentin, A. D. Wieck, A. Ludwig, A. Javadi, and R. J. Warburton, Nat. Phys. **19**, 857 (2023).
[26] Y.-X. Zhang and K. Mølmer, Phys. Rev. Lett. **125**, 253601 (2020).
[27] A. N. Poddubny, Phys. Rev. A **101**, 043845 (2020).
[28] B. Bakkensen, Y.-X. Zhang, J. Bjerlin, and A. S. Sørensen, arXiv:2110.06093.
[29] G. Calajó and D. E. Chang, Phys. Rev. Res. **4**, 023026 (2022).
[30] A. V. Poshakinskiy and A. N. Poddubny, Phys. Rev. A **108**, 023707 (2023).
[31] Y. Marques, I. A. Shelykh, and I. V. Iorsh, Phys. Rev. Lett. **127**, 273602 (2021).
[32] B. Schrinski, J. A. Brimer, and A. S. Sørensen, arXiv:2310.19115.
[33] X. Zhang, E. Kim, D. K. Mark, S. Choi, and O. Painter, Science **379**, 278 (2023).
[34] M. Scigliuzzo, G. Calajò, F. Ciccarello, D. Perez Lozano, A. Bengtsson, P. Scarlino, A. Wallraff, D. Chang, P. Delsing, and S. Gasparinetti, Phys. Rev. X **12**, 031036 (2022).
[35] M. Gong and e. a. Wang, Science **372**, 948 (2021).
[36] S.-P. Yu, J. A. Muniz, C.-L. Hung, and H. J. Kimble, Proc. Natl. Acad. Sci. U.S.A. **116**, 12743 (2019).
[37] N. V. Hauff, H. Le Jeannic, P. Lodahl, S. Hughes, and N. Rotenberg, Phys. Rev. Res. **4**, 023082 (2022).
[38] A. Sipahigil, R. E. Evans, D. D. Sukachev, M. J. Burek, J. Borregaard, M. K. Bhaskar, C. T. Nguyen, J. L. Pacheco, H. A. Atikian, C. Meuwly *et al.*, Science **354**, 847 (2016).
[39] L. Krinner, M. Stewart, A. Pazmiño, J. Kwon, and D. Schneble, Nature (London) **559**, 589 (2018).
[40] Y. Kim, A. Lanuza, and D. Schneble, arXiv:2311.09474.
[41] B. Windt, M. Bello, E. Demler, and J. I. Cirac, Phys. Rev. A **109**, 023306 (2024).
[42] I. Carusotto and C. Ciuti, Rev. Mod. Phys. **85**, 299 (2013).
[43] C. Noh and D. G. Angelakis, Rep. Prog. Phys. **80**, 016401 (2016).
[44] A. González-Tudela, A. Reiserer, J. J. García-Ripoll, and F. J. García-Vidal, Nat. Rev. Phys. **6**, 1 (2024).
[45] D. E. Chang, J. S. Douglas, A. González-Tudela, C.-L. Hung, and H. J. Kimble, Rev. Mod. Phys. **90**, 031002 (2018).
[46] Z. Wang, T. Jaako, P. Kirton, and P. Rabl, Phys. Rev. Lett. **124**, 213601 (2020).
[47] L. Leonforte, X. Sun, D. Valenti, B. Spagnolo, F. Illuminati, A. Carollo, and F. Ciccarello, arXiv:2402.10275.
[48] J. Rui, D. Wei, A. Rubio-Abadal, S. Hollerith, J. Zeiher, D. M. Stamper-Kurn, C. Gross, and I. Bloch, Nature (London) **583**, 369 (2020).
[49] K. Srakaew, P. Weckesser, S. Hollerith, D. Wei, D. Adler, I. Bloch, and J. Zeiher, Nat. Phys. **19**, 714 (2023).
[50] X. Huang, W. Yuan, A. Holman, M. Kwon, S. J. Masson, R. Gutierrez-Jauregui, A. Asenjo-Garcia, S. Will, and N. Yu, Prog. Quantum Electron. **89**, 100470 (2023).
[51] See Supplemental Material at http://link.aps.org/supplemental/10.1103/PhysRevLett.132.163602 for details about the derivation of the model, the characterizations of the interacting states, and the simulation of the system dynamics.
[52] H. J. Carmichael, *Statistical Methods in Quantum Optics 1* (Springer, Berlin Heidelberg, 1999).
[53] H.-P. Breuer and F. Petruccione, *The Theory of Open Quantum Systems* (Oxford University Press, Oxford, 2007).
[54] A. Asenjo-Garcia, M. Moreno-Cardoner, A. Albrecht, H. J. Kimble, and D. E. Chang, Phys. Rev. X **7**, 031024 (2017).
[55] A. González-Tudela, C.-L. Hung, D. E. Chang, J. I. Cirac, and H. J. Kimble, Nat. Photonics **9**, 320 (2015).
[56] A. González-Tudela and J. I. Cirac, Phys. Rev. A **96**, 043811 (2017).
[57] F. Galve and R. Zambrini, Phys. Rev. A **97**, 033846 (2018).
[58] A. González-Tudela and F. Galve, ACS Photonics **6**, 221 (2018).
[59] A. Albrecht, L. Henriet, A. Asenjo-Garcia, P. B. Dieterle, O. Painter, and D. E. Chang, New J. Phys. **21**, 025003 (2019).
[60] Y.-X. Zhang and K. Mølmer, Phys. Rev. Lett. **122**, 203605 (2019).
[61] J. Kumlin, K. Kleinbeck, N. Stiesdal, H. Busche, S. Hofferberth, and H. P. Büchler, Phys. Rev. A **102**, 063703 (2020).
[62] L. Ostermann, C. Meignant, C. Genes, and H. Ritsch, New J. Phys. **21**, 025004 (2019).
[63] J. A. Needham, I. Lesanovsky, and B. Olmos, New J. Phys. **21**, 073061 (2019).
[64] J. Zhong, N. A. Olekhno, Y. Ke, A. V. Poshakinskiy, C. Lee, Y. S. Kivshar, and A. N. Poddubny, Phys. Rev. Lett. **124**, 093604 (2020).
[65] D. F. Kornovan, N. V. Corzo, J. Laurat, and A. S. Sheremet, Phys. Rev. A **100**, 063832 (2019).
[66] B. Schrinski and A. S. Sørensen, New J. Phys. **24**, 123023 (2022).
[67] E. N. Economou, *Green's Functions in Quantum Physics* (Springer, Berlin, Heidelberg, 2006).
[68] O. A. Iversen and T. Pohl, Phys. Rev. Lett. **126**, 083605 (2021).
[69] S. J. Buckman and C. W. Clark, Rev. Mod. Phys. **66**, 539 (1994).
[70] R. J. Bettles, S. A. Gardiner, and C. S. Adams, Phys. Rev. Lett. **116**, 103602 (2016).
[71] E. Shahmoon, D. S. Wild, M. D. Lukin, and S. F. Yelin, Phys. Rev. Lett. **118**, 113601 (2017).

[72] M. T. Manzoni, M. Moreno-Cardoner, A. Asenjo-Garcia, J. V. Porto, A. V. Gorshkov, and D. E. Chang, New J. Phys. **20**, 083048 (2018).
[73] O. Rubies-Bigorda, V. Walther, T. L. Patti, and S. F. Yelin, Phys. Rev. Res. **4**, 013110 (2022).
[74] K. E. Ballantine and J. Ruostekoski, PRX Quantum **2**, 040362 (2021).
[75] C. C. Rusconi, T. Shi, and J. I. Cirac, Phys. Rev. A **104**, 033718 (2021).
[76] A. Asenjo-Garcia, J. D. Hood, D. E. Chang, and H. J. Kimble, Phys. Rev. A **95**, 033818 (2017).
[77] R. H. Lehmberg, Phys. Rev. A **2**, 883 (1970).
[78] H. T. Dung, L. Knöll, and D.-G. Welsch, Phys. Rev. A **57**, 3931 (1998).
[79] B. Bakkali-Hassani, C. Maury, Y.-Q. Zou, E. Le Cerf, R. Saint-Jalm, P. C. M. Castilho, S. Nascimbene, J. Dalibard, and J. Beugnon, Phys. Rev. Lett. **127**, 023603 (2021).
[80] C.-A. Chen and C.-L. Hung, Phys. Rev. Lett. **127**, 023604 (2021).
[81] T. Ozawa, H. M. Price, A. Amo, N. Goldman, M. Hafezi, L. Lu, M. C. Rechtsman, D. Schuster, J. Simon, O. Zilberberg, and I. Carusotto, Rev. Mod. Phys. **91**, 015006 (2019).
[82] G. Salerno, M. Di Liberto, C. Menotti, and I. Carusotto, Phys. Rev. A **97**, 013637 (2018).
[83] G. Salerno, G. Palumbo, N. Goldman, and M. Di Liberto, Phys. Rev. Res. **2**, 013348 (2020).
[84] L. W. Clark, N. Schine, C. Baum, N. Jia, and J. Simon, Nature (London) **582**, 41 (2020).
[85] J. Léonard, S. Kim, J. Kwan, P. Segura, F. Grusdt, C. Repellin, N. Goldman, and M. Greiner, Nature (London) **619**, 495 (2023).
[86] D. De Bernardis, Z.-P. Cian, I. Carusotto, M. Hafezi, and P. Rabl, Phys. Rev. Lett. **126**, 103603 (2021).
[87] D. De Bernardis, F. S. Piccioli, P. Rabl, and I. Carusotto, PRX Quantum **4**, 030306 (2023).
[88] C. Vega, D. Porras, and A. González-Tudela, Phys. Rev. Res. **5**, 023031 (2023).
[89] M. Bello and J. I. Cirac, Phys. Rev. B **107**, 054301 (2023).
[90] J. Perczel, J. Borregaard, D. E. Chang, H. Pichler, S. F. Yelin, P. Zoller, and M. D. Lukin, Phys. Rev. Lett. **119**, 023603 (2017).
[91] J. Perczel, J. Borregaard, D. E. Chang, H. Pichler, S. F. Yelin, P. Zoller, and M. D. Lukin, Phys. Rev. A **96**, 063801 (2017).
[92] J. Perczel, J. Borregaard, D. E. Chang, S. F. Yelin, and M. D. Lukin, Phys. Rev. Lett. **124**, 083603 (2020).
[93] E. J. Bergholtz and Z. Liu, Int. J. Mod. Phys. B **27**, 1330017 (2013).
[94] G. Semeghini, H. Levine, A. Keesling, S. Ebadi, T. T. Wang, D. Bluvstein, R. Verresen, H. Pichler, M. Kalinowski, R. Samajdar, A. Omran, S. Sachdev, A. Vishwanath, M. Greiner, V. Vuletić, and M. D. Lukin, Science **374**, 1242 (2021).
[95] K. Brechtelsbauer and D. Malz, Phys. Rev. A **104**, 013701 (2021).
[96] F. Andreoli, B. Windt, S. Grava, G. M. Andolina, M. J. Gullans, A. A. High, and D. E. Chang, arXiv:2303.10998.